Title

Insights into the mechanism of oligodendrocyte protection and remyelination enhancement by the integrated stress response.

Journal

Glia, 71(9)

Authors

Chen, Yanan
Quan, Songhua
Patil, Vaibhav
et al.

Publication Date

2023-09-01

DOI

10.1002/glia.24386

Peer reviewed

HHS Public Access

Author manuscript

Glia. Author manuscript; available in PMC 2024 September 01.

Published in final edited form as:

Glia. 2023 September ; 71(9): 2180–2195. doi:10.1002/glia.24386.

Insights into the mechanism of oligodendrocyte protection and remyelination enhancement by the integrated stress response

Yanan Chen[*,1], **Songhua Quan**[2], **Vaibhav Patil**[2], **Rejani B. Kunjamma**[2], **Haley M. Tokars**[2], **Eric D. Leisten**[2], **Godwin Joy**[1], **Samantha Wills**[1], **Jonah R. Chan**[3], **Yvette C. Wong**[2], **Brian Popko**[*,2]

[1]Deptment of Biology, Loyola University Chicago, Chicago, IL, 60660, USA.

[2]Department of Neurology, Northwestern University, Feinberg School of Medicine, Chicago, IL 60611, USA.

[3]Weill Institute for Neuroscience, Department of Neurology, University of California, San Francisco, CA, 94158, USA.

Abstract

CNS inflammation triggers activation of the integrated stress response (ISR). We previously reported that prolonging the ISR protects remyelinating oligodendrocytes and promotes remyelination in the presence of inflammation. However, the exact mechanisms through which this occurs remain unknown. Here, we investigated whether the ISR modulator Sephin1 in combination with the oligodendrocyte differentiation enhancing reagent bazedoxifene (BZA) is able to accelerate remyelination under inflammation, and the underlying mechanisms mediating this pathway. We find that the combined treatment of Sephin1 and BZA is sufficient to accelerate early-stage remyelination in mice with ectopic IFN-γ expression in the CNS. IFN-γ, which is a critical inflammatory cytokine in multiple sclerosis (MS), inhibits oligodendrocyte precursor cell (OPC) differentiation in culture and triggers a mild ISR. Mechanistically, we further show that BZA promotes OPC differentiation in the presence of IFN-γ, while Sephin1 enhances the IFN-γ-induced ISR by reducing protein synthesis and increasing RNA stress granule formation in differentiating oligodendrocytes. Finally, pharmacological suppression of the ISR blocks stress granule formation *in vitro* and partially lessens the beneficial effect of Sephin1 on disease progression in a mouse model of MS, experimental autoimmune encephalitis (EAE). Overall, our findings uncover distinct mechanisms of action of BZA and Sephin1 on oligodendrocyte lineage cells under inflammatory stress, suggesting that a combination therapy may effectively promote restoring neuronal function in MS patients.

[*]Co-Corresponding Authors: Yanan Chen, Ph.D. Department of Biology, Loyola University Chicago, 1032 W. Sheridan Rd, Chicago, IL 60660, ychen55@luc.edu, Brian Popko, Ph.D. Department of Neurology, Northwestern University, Feinberg School of Medicine, 320 East Superior Ave, Chicago, IL 60611, brian.popko@northwestern.edu.

COMPETING INTERESTS

BP is an inventor on US Patent #10,905,663 entitled “Treatment of Demyelinating Disorders” that describes a small molecule approach to enhancing the ISR as a therapeutic approach for demyelinating disorders. The structure of Sephin1 is included in the molecules covered. BP is also member of the scientific advisory board of Inflectis Bioscience. JRC has received personal compensation for consulting from Inception Sciences (Inception 5) and Pipeline Therapeutics Inc, and has contributed to and received personal compensation for a US Provisional Patent Application concerning the use of BZA as a remyelination therapy (US Provisional Patent Application Serial Number 62/374,270 (issued 08/12/2016)).

Graphical Abstract

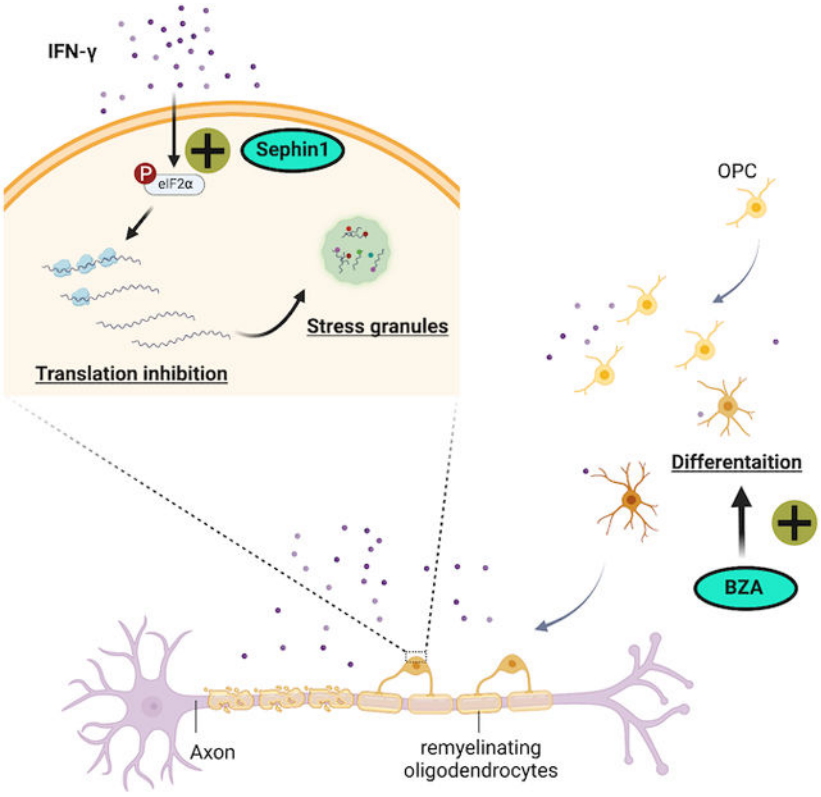

Keywords

Integrated stress response; multiple sclerosis; remyelination

INTRODUCTION

Multiple sclerosis (MS) is an immune-mediated demyelinating disease that causes neurological impairment and frequently results in significant disability (Compston and Coles, 2002; Frohman et al., 2006; Reich et al., 2018). Although the etiology of MS is still unknown, the consensus is that central nervous system (CNS) inflammation is a major driver of MS pathology. It is well accepted that activated autoreactive myelin-specific T cells migrate into the CNS, are reactivated locally, and release cytokines leading to oligodendrocyte and myelin damage (Lassmann, 2014, 2018; Titus et al., 2020).

Oligodendrocytes produce a vast amount of myelin membrane and thus are particularly sensitive to cellular homeostatic changes that result from diverse stresses, including CNS inflammation (Clayton and Popko, 2016; Lin and Popko, 2009; Volpi et al., 2016). To cope with inflammatory stress, an innate cytoprotective response called the integrated stress response (ISR) is triggered in oligodendrocytes, centered by the phosphorylation of the eukaryotic translation initiation factor 2 alpha (eIF2α) (Pakos-Zebrucka et al., 2016; Way and Popko, 2016; Way et al., 2015). Phosphorylated eIF2α (p-eIF2α) inhibits

the activity of eukaryotic translation initiation factor 2B (eIF2B), and diminishes global translation by preventing ternary complex formation, thus reducing the protein load on the endoplasmic reticulum (ER). Concurrently, p-eIF2α selectively upregulates translation of chaperones and protective proteins, including the activating transcription factor 4 (ATF4), ATF5, C/EBP homologous protein (CHOP), and protein growth arrest and DNA-damage inducible (GADD34), aiding cellular survival and recovery (Zhang and Kaufman, 2008). GADD34 is recruited to protein phosphatase 1 (PP1), which dephosphorylates p-eIF2α ensuring translation re-initiation. Previous genetic studies showed that ISR activation in oligodendrocytes protected myelinating and remyelinating oligodendrocytes against inflammatory attack (Lin et al., 2013, 2014). Sephin1, a recently-identified small molecule, is able to prolong the ISR by inhibiting GADD34-PP1c complex activity, thereby prolonging the phosphorylation of eIF2α (Crespillo-Casado et al., 2017; Das et al., 2015). We previously showed that Sephin1 protects oligodendrocytes against inflammatory stress in a mouse model of MS, experimental autoimmune encephalomyelitis (EAE) (Chen et al., 2019). However, the exact mechanism by which Sephin1 protects oligodendrocytes from inflammation remains unknown.

Remyelination is known to be incomplete in MS as remyelinating oligodendrocytes, both pre-existing and newly formed, are challenged by an inflammatory environment (Ruffini et al., 2004). Inflammation diminishes the capacity of oligodendrocyte precursor cells (OPCs) to develop into mature oligodendrocytes and remyelinate demyelinated lesions (Franklin and Ffrench-Constant, 2008; Starost et al., 2020). The T cell cytokine interferon-gamma (IFN-γ) is considered to be a critical inflammatory mediator of MS pathogenesis (Patel and Balabanov, 2012). Using *GFAP-tTA; TRE-IFN-γ* transgenic mice in which IFN-γ is secreted in a doxycycline (dox)-dependent manner from astrocytes, we have previously shown that IFN-γ expression in the CNS suppresses remyelination following cuprizone-induced oligodendrocyte toxicity. However, prolonging the ISR through Sephin1 treatment or mutating GADD34 protects remyelinating oligodendrocytes and increases the level of remyelination (Chen et al., 2021). In the same inflammatory demyelination/remyelination model, we have also shown that combining Sephin1 with the oligodendrocyte differentiation enhancing reagent bazedoxifene (BZA) further increases myelin thickness, but not the number of remyelinating oligodendrocytes or remyelinated axons (Chen et al., 2021). Nevertheless, whether the combined treatment is able to accelerate remyelination under inflammatory conditions remains untested and the underlying mechanisms of the observed effects have not been fully elucidated.

Here, we investigated the remyelination effect of Sephin1 and BZA at an early stage of remyelination using the *GFAP-tTA; TRE-IFN-γ* transgenic mouse model along with cuprizone-induced demyelination. We demonstrate that the combined treatment of Sephin1 and BZA show an additive effect on promoting early-stage remyelination in the presence of inflammation. Using primary OPC cultures exposed to IFN-γ, we further show that BZA promotes OPC differentiation while Sephin1 boosts the IFN-γ-induced ISR by reducing protein synthesis and increasing RNA stress granule formation in the differentiating cells. In addition, we provide evidence that eIF2B activators reduce stress granule formation and partially blunt the beneficial effect of the ISR enhancer Sephin1 on EAE disease progression. Collectively, our results illustrate that Sephin1's mechanism is distinct from

that of BZA to protect oligodendrocytes against inflammation by inhibiting translation initiation and activating stress granule formation.

RESULTS

Combined treatment of Sephin1 and BZA accelerates early-stage remyelination in the presence of IFN-γ

In our previous study, using a *GFAP-tTA;TRE-IFN-γ* double-transgenic mouse model of cuprizone demyelination/remyelination, we did not observe additional benefits from the combined treatment of Sephin1 and BZA on the number of oligodendrocytes and remyelinated axons present at three weeks after cuprizone withdrawal (Chen et al., 2021). However, given that remyelination in the treatment groups had already reached pre-lesion levels after three weeks of remyelination, we reasoned that examining earlier recovery time-points might reveal differences in the treatment groups. Thus, to examine whether the combined treatment confers any benefit at an earlier stage of remyelination, we utilized the same *GFAP-tTA;TRE-IFN-γ* double-transgenic mouse model along with cuprizone exposure (Chen et al., 2021; Lin et al., 2006). We removed the doxycycline (Dox) chow to induce CNS expression of IFN-γ and placed the mice on a diet of 0.2% cuprizone chow to trigger demyelination at six weeks of age (Figure 1a). Sephin1 (8 mg/kg, i.p.) and/or BZA (10 mg/kg, gavage) were administered daily to the mice beginning three weeks after starting the cuprizone diet, which represents a point of peak demyelination. After five weeks of cuprizone exposure, the mice were placed back on a normal diet for two weeks (Figure 1a). Only mice with the highest level of IFN-γ expression in the CNS were selected for further examination at two weeks after cuprizone withdrawal (Supplementary figure 1a). Both the Sephin1 group and the combined Sephin1/BZA group (*$p<0.05$) presented with an increased number of remyelinated axons in the corpus callosum when examined by electron microscope, suggesting that ISR enhancement by Sephin1 at least partially drives the early stages of remyelination (Figure 1b,c). This is in contrast to our previous finding at the late-stages of remyelination, 3 weeks after cuprizone withdrawal, during which both individual and combined treatments displayed more remyelinated axons than the vehicle group (Chen et al., 2021). Moreover, although no significant difference was detected in MBP immunofluorescent intensity (Supplementary figure 1b, c), the g-ratios of myelinated axons were significantly lower in the combination treatment group than the vehicle-treated group (*$p<0.05$) and single treatment groups (**$p<0.01$ vs Sephin1, *$p<0.05$ vs BZA) (Figure 1b,c), indicating that axons of the combination treated mice had thicker myelin.

We also examined the status of remyelinating oligodendrocytes after two weeks. Using immunofluorescent staining, we found that mice receiving combined Sephin1/BZA and individual BZA treatment had more CC1+ mature oligodendrocytes than vehicle treatment (*$p<0.05$) in the corpus callosum of the IFN-γ expressing mice (Figure 2a,b). Interestingly, the intensity of phosphorylated eIF2α (p-eIF2α) was significantly increased in CC1+ oligodendrocytes when treated with Sephin1 or Sephin1/BZA rather than with vehicle, suggesting that Sephin1 enhanced the ISR in remyelinating oligodendrocytes in the presence of IFN-γ (Figure 2a,c). Together, these findings indicate that the combined treatment of

Sephin1 and BZA drives the remyelination process in the presence of IFN-γ faster than either treatment alone.

Combined treatment of Sephin1 and BZA does not affect OPC proliferation but promotes OPC differentiation in the presence of IFN-γ

Remyelination is a regenerative process that requires the recruitment and proliferation of oligodendrocyte progenitor cells (OPCs) to demyelinated areas. This is followed by their differentiation into mature remyelinating oligodendrocytes to form functional myelin sheaths (Franklin and Ffrench-Constant, 2008). To determine whether the combined treatment of Sephin1 and BZA promotes OPC proliferation, we examined the corpus callosum of the IFN-γ expressing mice with the OPC marker PDGFRα and the proliferation marker Ki67 at two weeks of remyelination. Combined or individual treatments of Sephin1 and BZA had no effect on the number of total OPCs or proliferative OPCs (PDGFRα+ and Ki67+) in the demyelinated lesions (Figure 3a,b). Next, we interrogated the influence of Sephin1 and BZA on differentiation of OPCs isolated from postnatal mouse pups with or without the exposure of IFN-γ *in vitro*. Significantly fewer OPCs differentiated into MBP+ oligodendrocytes in the cultures exposed to IFN-γ (+IFN-γ; NT) than non-IFN-γ treated cultures (-IFN-γ; NT) (#$p<0.05$, unpaired t test) after 24 hours (Figure 3c,d). Interestingly, when treated with Sephin1 (+IFN-γ; Seph), OPC differentiation reached the control level of non-IFN-γ (-IFN-γ; NT) cultures (Figure 3c,d). These data suggest that OPC differentiation is inhibited by IFN-γ, while Sephin1 permits OPC differentiation in the presence of IFN-γ. Combined Sephin1/BZA and BZA alone, however, promoted OPCs to differentiate into MBP+ oligodendrocytes both in the absence and presence of IFN-γ (*$p<0.05$ vs BZA, **$p<0.01$ vs Sephin1/BZA, Figure 3c,d). No additional difference was observed between the combination Sephin1/BZA treatment and individual BZA treatment. Similar results were found after 48 hours and 72 hours of treatment (Supplement figure 2). Overall, this data shows that Sephin1 permits OPC differentiation in the presence of inflammatory stress, while BZA promotes OPC differentiation in control or inflammatory conditions.

eIF2α phosphorylation induction by IFN-γ results in mild protein synthesis inhibition in oligodendrocytes

Before exploring the influence of Sephin1 on stressed oligodendrocytes, we first needed to better understand the inflammatory environment surrounding oligodendrocytes and other CNS resident cells. T-cell secreted IFN-γ is considered to be a critical inflammatory mediator in MS (Patel and Balabanov, 2012). Both our *in vivo* and *in vitro* models incorporated IFN-γ to mimic the inflammatory environment of MS. Previously, our studies have shown that IFN-γ activates the ISR in differentiating OPCs as indicated by increased p-eIF2α levels (Chen et al., 2019; Lin et al., 2005). However, the downstream molecular mechanisms by which IFN-γ influences oligodendrocytes remain unclear.

First, we exposed purified differentiating OPCs to IFN-γ or a well-known ER stressor thapsigargin (TG) and compared the expression of downstream targets of the ISR by Western-blot. TG induces ER stress by inhibiting Ca^{2+}-ATPase and thereby disturbing ER calcium homeostasis (Lytton et al., 1991; Sehgal et al., 2017). Levels of p-eIF2α significantly increased rapidly with the TG treatment, peaking at one hour (***$p<0.0001$)

(Figure 4a,c). Similarly, IFN-γ increased p-eIF2α expression but at a much slower rate, starting at eight hours (***p<0.0001) and peaking at 20 hours (p<0.0001) (Figure 4b,d). We also examined downstream stress-induced ISR signaling components, which aid in cell survival and recovery. ATF4, GADD34, CHOP, and BIP levels in oligodendrocytes significantly increased after two hours of TG treatment, indicating a fully activated ISR (Figure 4e,g). The levels were comparable to those observed in positive control NIH 3T3 cells treated with TG. Surprisingly, IFN-γ treatment did not alter the expression of these ISR components at any of the time points examined (Figure 4f,h).

Phosphorylation of eIF2α mediates translational control, causing an overall reduction in translation initiation. To examine the effect of p-eIF2α caused by IFN-γ on protein synthesis, we utilized a puromycin assay based on the structural resemblance between puromycin and the 3' end of aminoacylated tRNA (aa-tRNA). We added puromycin to cultured OPCs, where puromycin instead of aa-tRNA entered the ribosome's A-site and accepted the nascent peptide chain, leading to translation termination and the release of nascent chains bearing a 3' puromycin. These puromycilated peptides were detected by Western-blots using anti-puromycin antibodies, generating a laddering pattern that reflects newly synthesized proteins (Schmidt et al., 2009). Following the pattern of p-eIF2α levels, TG significantly reduced puromycin incorporated protein synthesis at one hour (***p<0.001) and two hours of treatment (***p<0.001) (Figure 5a,c). Surprisingly, Western blot analysis did not reveal any changes in protein synthesis in IFN-γ treated oligodendrocytes (Figure 5b,d). We thereby employed a more sensitive method to better detect nascent protein synthesis in situ with an alkyne analog of puromycin, O-propargyl-puromycin (OP-puro) and a fluorescent azide (Figure 6e) (Liu et al., 2012). OP-puro incorporates into nascent polypeptides, which are detected by copper (I)-catalyzed azide-alkyne cycloaddition (CuAAC) with Alexa568-azide. As expected, treatment with a protein synthesis inhibitor cycloheximide (CHX) significantly reduced the fluorescent intensity of Alexa568 (****p<0.0001) (Figure 6e,f). Compared to the untreated control (CTL) at eight hours, a significant decrease of fluorescent intensity was found in IFN-γ treated cells, suggesting a reduction of newly synthesized proteins (****p<0.0001) (Figure 6e,f).

In addition, to determine whether IFN-γ interferes with ISR activation caused by ER stress, we also treated cells with a combination of IFN-γ and TG. We found that TG was still capable of inducing eIF2α phosphorylation and reducing protein synthesis in the presence of IFN-γ (***p<0.001) (Supplementary figure 3). Overall, these data indicate that a mild ISR is activated in oligodendrocytes in response to the presence of IFN-γ.

Sephin1 induces translation reduction in IFN-γ stressed oligodendrocytes by upregulating the phosphorylation of eIF2α and the formation of RNA stress granules

Previously, we showed that Sephin1 prolongs eIF2α phosphorylation in IFN-γ-stressed oligodendrocytes *in vivo* (Chen et al., 2019). Here, we also observed increased p-eIF2α in remyelinating oligodendrocytes of IFN-γ expressing mice treated with Sephin1 (Figure 2a,c). This prolonged phosphorylation of p-eIF2α during inflammatory stress via Sephen1 may provide protection to oligodendrocytes, but the downstream molecular mechanism is unclear. We therefore examined p-eIF2α levels and protein synthesis in

IFN-γ-exposed OPCs treated with Sephin1 by immunoblotting. Sephin1 further increased the phosphorylation of eIF2α in IFN-γ stressed oligodendrocytes at eight hours and significantly at 20 hours (*p<0.05) (Figure 6a,b). Strikingly, Sephin1 also significantly lessened protein synthesis in these cells at 20 hours (*p<0.05) (Figure 6c,d). In addition, Sephin1 reduced protein synthesis while enhancing the level of p-eIF2α in TG-stressed oligodendrocytes (Figure 6a-d). Of note, using the sensitive OP-puro assay, we observed a reduction of fluorescent intensity in IFN-γ (****p<0.0001) or Sephin1 treated cells (****p<0.0001) at eight hours of treatment (Figure 6e,f), suggesting that cells are under mild stress with both individual treatments. Nevertheless, consistent with the Western blot results (Figure 6c,d), Sephin1 further reduced the fluorescent signals of newly formed peptides in IFN-γ stressed oligodendrocytes (**p<0.01) (Figure 6e,f).

A full-blown ISR reduces the levels of overall protein synthesis, while activating translation of a set of mRNA molecules encoding for transcription factors and other cytoprotective proteins. Given that p-eIF2α levels were increased by Sephin1, we examined the expression levels of downstream components of the ISR. Although there was not a significant increase in ATF4 expression, the levels of GADD34 were increased after 24 hours of Sephin1 treatment in IFN-γ stressed oligodendrocytes (Supplementary figure 4). We also examined the expression levels of downstream targets of other arms of the unfolded protein response (UPR), including *Bip*, a downstream target of the ATF6a pathway, as well as *Xbp1s*, a target of the IRE/XBP1s pathway. Western blot did not detect any increase in the expression of BIP and XBP1s with either IFN-γ or IFN-γ + Sephin1 treatment (Supplementary figure 4).

Translation inhibition by phosphorylation of eIF2α generates ribosome-free mRNA that becomes sequestered into RNA stress granules (Glauninger et al., 2022; Hofmann et al., 2021; Kedersha et al., 1999). To identify if stress granule assembly occurs in oligodendrocytes treated with TG or IFN-γ ± Sephin1, we stained treated oligodendrocytes at different timepoints with the RasGAP SH3-domain-binding protein 1 (G3BP1), a key component for stress granule formation (Tourrière et al., 2003). G3BP1 was present diffusively in the cytoplasm of cultured oligodendrocytes without treatment (CTL), but clearly formed granules were present in sodium arsenite as well as TG treated cells after one hour (Figure 7a). In contrast, G3BP1 granules were not found in cells that were exposed for one or eight hours to IFN-γ (Figure 7a, b). Remarkably, distinct G3BP1 positive granules appeared in oligodendrocytes exposed to both IFN-γ and Sephin1 after eight hours (Figure 7b). Stress granules were dispersed by 20 or 48 hours of exposure to the dual treatment (Supplementary figure 5a). To further confirm the presence of stress granules, we assessed the G3BP1 stress granules by super-resolution microscopy (Structured Illumination Microscopy, SIM). Here too, we observed G3BP1 granules only in cells treated with both IFN-γ and Sephin1 at the eight- and 16-hour timepoints (**p<0.01, *p<0.05) (Figure 7c, d; Supplementary figure 5b). Moreover, we observed more stress granule containing-remyelinating oligodendrocytes *in vivo* in IFN-γ expressing mice treated with Sephin1 than in vehicle treated mice (*p<0.05) (Supplementary figure 6). Based on the observation above, we infer that Sephin1 promotes oligodendrocytes survival under inflammatory attack by further reducing protein synthesis and/or promoting stress granule assembly.

eIF2B activators counteract the effect of Sephin1 on IFN-γ stressed oligodendrocytes and on EAE

Phosphorylated eIF2α acts as a competitive inhibitor of eIF2B, which slows protein synthesis (Krishnamoorthy et al., 2001). A highly selective eIF2B activator, ISRIB (for ISR inhibitor), has been shown to blunt the ISR by antagonizing the inhibitory effect of p-eIF2α on eIF2B (Sidrauski et al., 2015). We therefore hypothesized that if Sephin1 promotes stress granule assembly by enhancing the ISR, this effect could be inhibited by ISRIB. We found that diffusively distributed G3BP1 staining presented in oligodendrocytes treated with only ISRIB for eight hours (Figure 8a). The number of cells with G3BP1 positive granules was significantly increased in cells exposed to both IFN-γ and Sephin1 (IFN-γ+Seph, *$p<0.05$) compared to the control, while adding ISRIB to the cell culture media reduced the formation of stress granules (IFN-γ+Seph+ISRIB, *$p<0.05$) (Figure 8a,b; Supplementary figure 5b).

In addition, we hypothesized that if Sephin1 protects oligodendrocytes from inflammation by prolonging ISR-induced elevated levels of p-eIF2α, this effect could be inhibited by 2BAct, a CNS penetrant eIF2B activator (Wong et al., 2019). To test this, we conducted daily Sephin1 treatments on EAE mice provided with normal chow or chow containing 2BAct. As previously reported (Chen et al., 2019), Sephin1 delayed the onset of EAE peak symptoms (Figure 8c). In contrast, Sephin1 treated mice fed chow containing 2BAct developed EAE symptoms significantly faster than those on normal chow (at PID 15 and PID 16; *$p<0.05$) (Figure 8c), although the beneficial impact of Sephin1 was not completely abrogated by 2BAct. These findings further attest that Sephin1 provides CNS protection against inflammation by enhancing the ISR.

DISCUSSION

In this study, we have shown that the combination of Sephin1 and BZA accelerates the remyelination process faster than Sephin1 or BZA individually in the presence of an adverse environment created by the inflammatory cytokine IFN-γ. Our results indicate that this additive effect is derived from Sephin1 and BZA's complementary mechanisms of action on the remyelinating oligodendrocyte lineage cells. We show that BZA promotes OPC differentiation in the presence of IFN-γ, whereas Sephin1 permits oligodendrocyte development in these conditions. Moreover, our results indicate that Sephin1 extends the level of IFN-γ triggered ISR by enhancing p-eIF2α levels, which leads to reduced overall protein synthesis and the formation RNA stress granules. In addition, we show that an ISR suppressor 2BAct, which reverses the effects of p-eIF2α, can partially block the protective effects of Sephin1 on EAE, indicating that Sephin1 safeguards oligodendrocytes against inflammation by enhancing the ISR. Our observation that the combined treatment of Sephin1 and BZA resulted in more rapid and robust remyelination in the presence of inflammation is critical because remyelination provides protection against axonal degeneration secondary to demyelination. More rapid remyelination is likely to preserve more axons.

Remyelination restores neuronal function and prevents axonal degeneration, but remyelination is either incomplete or absent in MS (Fancy et al., 2010; Franklin and Goldman, 2015; Schultz et al., 2017). Efforts to promote remyelination have largely

focused on promoting OPC differentiation into remyelinating oligodendrocytes (Franklin and Simons, 2022; Franklin et al., 2021). Nevertheless, stimulating repair is challenging in the hostile environment created by CNS inflammation, during which OPC differentiation efficacy largely declines (Franklin and Ffrench-Constant, 2017; Galloway et al., 2020). BZA, a third-generation selective estrogen receptor modulator, has been found to enhance OPC differentiation in response to focal demyelination, independent of it estrogen receptor (Rankin et al., 2019). In our recent study, we found that BZA promotes remyelination in an inflammatory remyelination model as well (Chen et al., 2021). Here, we further showed that BZA can promote OPC differentiation in an inflammatory milieu and that remyelination is further accelerated by the ISR modulator Sephin1.

In our inflammatory demyelination/remyelination model, we utilized IFN-γ as the inflammatory stressor. However, the mechanism by which IFN-γ leads to oligodendrocyte abnormalities remains poorly understood. It has been well documented that the T-cell-derived pleiotropic cytokine IFN-γ plays a critical, albeit complex, role in the development and progression of MS and EAE (Goverman, 2009; Lees and Cross, 2007; Lin et al., 2007; Popko et al., 1997). We previously reported that the inhibitory effects of IFN-γ on the remyelination process are associated with an activated stress response in oligodendrocytes, although the mechanisms are unclear (Lin et al., 2006). ISR induction not only reduces global protein synthesis but also promotes translation of a set of cytoprotective proteins (Holcik and Sonenberg, 2005; Zhang and Kaufman, 2008). Here, we observed significant eIF2α phosphorylation and slight inhibition of global protein synthesis in cells exposed to IFN-γ, but no increase in the level of translation of ISR-inducible proteins (Figure 4–6). It is likely that IFN-γ induces a mild ISR that decreases the ternary complex concentration without activating a full downstream ISR response (Cagnetta et al., 2019). Cells may also employ additional cell responses other than the ISR to tackle IFN-γ stress, such as the UPR. The UPR not only converges with the ISR through p-eIF2α, but also induces ISR-independent arms, whereby the transcription factors ATF6 and the spliced form of X-box binding protein 1 (XBP1s) increase expression of genes that reinstate ER homeostasis (Costa-Mattioli and Walter, 2020). Activation of ATF6 but not XBP1s in oligodendrocytes, was reported in EAE (Hussien et al., 2015; Mháille et al., 2008; Stone and Lin, 2015). ATF6 deficiency was shown to exacerbates ER stress-induced oligodendrocyte death in the developing CNS of IFN-γ-expressing mice (Stone et al., 2018). In this study, we did not observe any upregulated expressions of the downstream targets of either the ATF6 or XBP1s pathways in IFN-γ-stressed oligodendrocytes.

Our data shows that BZA combined with Sephin1 exhibited a faster recovery by increasing remyelinated axons and myelin thickness than the single treatment of BZA. This directed our focus to how Sephin1 promotes remyelination in an inflammatory environment. Sephin1 had little impact on OPC proliferation and differentiation. Therefore, we posit that Sephin1 provides protection to surviving and newly formed oligodendrocytes against inflammation. Although the exact mechanism of how Sephin1 enhances p-eIF2α is controversial (Carrara et al., 2017; Crespillo-Casado et al., 2018), our findings indicate that it enhances the ISR response by increasing p-eIF2α levels in remyelinating oligodendrocytes in the presence of an inflammatory environment. Most importantly, our study uncovers the downstream pathways following ISR enhancement by Sephin1 in oligodendrocytes. We show that

Sephin1 elevated the IFN-γ induced p-eIF2α levels, resulting in a reduction of overall protein synthesis, which is protective (Pavitt and Ron, 2012).

Our observation of RNA stress granule formation in IFN-γ stressed cells when treated with Sephin1 helps shed light on the mechanism of Sephin1's cytoprotective effect. It is widely believed that stress granules are sites of mRNA sequestering during cellular stress (Anderson and Kedersha, 2008; Kedersha and Anderson, 2002). Although stress granules do not directly repress global translation (Khong et al., 2017; Mateju et al., 2020), emerging evidence indicates that stress granules promote cellular survival in diverse disease states by protecting mRNA and proteins from degradation, minimizing energy expenditure, acting in translational quality control, and sequestering proapoptotic factors (Glauninger et al., 2022). Our findings, along with previous evidence, raise the possibility that Sephin1's protective effect on oligodendrocytes is correlated with RNA stress granule formation in response to phosphorylation of eIF2α. Notably, eIF2B activators, ISRIB and 2BAct, blocked the effect of Sephin1 *in vitro* and *in vivo,* respectively, further supporting our proposed protective mechanism of Sephin1.

In summary, we observed a significant recovery benefit from the combined treatment of Sephin1 and BZA on inflammatory remyelination and unveiled distinct mechanisms of Sephin1 and BZA on oligodendrocyte lineage cells that underscore this additive effect. These findings have important implications for promoting the ensheathment of demyelinated axons and restoring neuronal function, especially in an inflammatory environment, thereby offering the potential to delay, prevent, or reverse the neurological pathologies of MS. These results should be informative as neuroprotective and neuroreparative therapeutic strategies are being developed for MS and other CNS inflammatory demyelinating disorders.

MATERIALS AND METHODS

Animal and drug treatment

Animal use and drug administration were described in our previous study (Chen et al., 2021). GFAP-tTA mice on a C57BL/6J background were mated with TRE-IFN-γ mice on a C57BL/6J background to produce GFAP-tTA; TRE-IFN-γ double-transgenic mice. These mice were given 200 ppm Dox (Envigo, Madison, WI) from conception to prevent transcriptional activation of IFN-γ. The Dox diet was discontinued and replaced with a 0.2% cuprizone diet (Envigo, Madison, WI) starting at six weeks of age. Cuprizone feeding lasted five weeks and then the mice were placed back on normal chow for up to two weeks to allow early remyelination to occur. Concurrently, 8 mg/kg of Sephin1 (i.p.) (#SM1356, Sigma, St. Louis, MO) or 10 mg/kg of BZA (gavage) (#PZ0018, Sigma) were given daily to the GFAP-tTA; TRE-IFN-γ mice, starting from three weeks of cuprizone exposure. Equal number of male and female mice were used in each experiment group. The corpus callosum of each mouse was collected two weeks after cuprizone feeding cessation.

EAE was induced in 9-week-old female C57BL/6J mice (Jackson Laboratories, Bar Harbor, ME) by subcutaneous flank administration of 200 μg MOG35–55 peptide emulsified with complete Freund's adjuvant (CFA) and killed Mycobacterium tuberculosis H37Ra (#EK2100 kit, Hookes Laboratory, Lawrence, MA). Intraperitoneal (i.p.) injections of 200

ng pertussis toxin were given immediately after administration of the MOG emulsion and again 24 hours later. Mice were blindly scored daily for clinical signs of EAE from 0 (no symptoms) to 5 (most severe). Mice were put on a 2BAct diet, which was generously provided by Dr. Carmela Sidrauski's group (Calico Life Sciences, South San Francisco, CA), two days before EAE induction. Daily treatment with i.p Sephin1 at 8mg/kg were started seven days after EAE induction. The treatment of the animals used in this study was conducted in accordance with the ARRIVE guidelines and in complete compliance with the Animal Care and Use Committee guidelines of Northwestern University.

OPC isolation and cell culture

Oligodendrocyte precursor cells (OPCs) were isolated and purified following a previously described method (Dugas and Emery, 2013). Briefly, mice brain cortices from 6–7 days old pups were collected, diced, and digested with papain (# 9001734, Worthington, Lakewood, NJ) at 37ºC. Cells were triturated, suspended, and sequentially immunopanned at room temperature on plates coated with Ran-2, GalC, and O4 antibodies from a hybridomal supernatant. OPCs sticking to the O4 coated plate were trypsinized and seeded on poly-D-Lysine (pDL)-coated plates in growth media. To get sufficient amount OPCs, the cells were split and plated twice in growth media to proliferate. NIH 3T3 fibroblast cell line was purchased from ATCC (# CRL-1658) and cultured in DMEM with 10% bovine calf serum and 1% penicillin-streptomycin.

Puromycin incorporation assays

After OPCs were incubated in differentiation media overnight, the cells were treated 200 U/ml of IFN-γ (#485-MI-100, R&D, Minneapolis, MN), and/or 200 nM of thapsigargin (TG, #67526958, Sigma) with or without Sephin1 (50 μM, Sigma) as designated regimens. OPCs were seeded on PDL-coated plates in growth media. One day later, the media were changed to differentiation media and the cells were incubated at 37ºC overnight. On the next day, cells were either untreated or treated with IFN-γ or TG, as described above. For puromycin labeling, puromycin (10 μg/ml, Sigma) were added during the last 30 min before harvest.

Western blot

OPCs were washed twice with PBS and lysed in ice-cold RIPA buffer (Sigma) containing Halt Protease and Phosphatase Inhibitor Cocktail (#PI78441, Thermo Fisher Scientific). Lysates were then centrifuged at 12,000 rpm for 20 min at 4ºC. A total 20 μg of protein lysates was separated by 4–12% SDS-PAGE (Bio-Rad, 4561095) and transferred to a nitrocellulose membrane. The following primary antibodies were used: anti-p-eIF2α (Abcam, ab32157, 1:2000), anti-T-eIF2α (Cell Signaling, 9722s, 1:1000), anti-puromycin (Millipore, MABE343, 1:2000), anti-BIP (Cell Signaling, 3177s, 1:1000), anti-GADD34 (Proteintech, 10449–1-AP, 1:500), anti-ATF4 (Santa Cruz, sc-390063, 1:500), anti-CHOP (Thermo Fisher, MAI-250, 1:500), anti-XBP-1-spliced (Cell Signaling, 82914s, 1:1000), and anti-actin (Sigma, A2066, 1:2000). Quantification of Western blot bands were performed by Image Lab Software (Bio-Rad).

Cell treatments and Immunocytochemistry

OPCs were grown on PDL-coated 4-well glass culture slides (BD, 354104). To study OPC differentiation, we exchanged medium to one without differentiation factors (T3) and exposed cells to 200 U/ml IFN-γ with the treatment of 500 nm BZA (#PZ0018, Sigma), and/or 50 uM Sephin1 (a gift from InFlectis Biosciences) for 24, 48 and 72 hrs. To induce cellular stress, cells were treated for one hour with 500 μM sodium arsenite (#S7400, Sigma), 200 nM TG, or 200 U/ml IFN-γ. A longer treatment was conducted for 8, 16, 24, or 48 hours with 200 U/ml IFN-γ, 5μM ISRIB (#SML0843, Sigma), and/or 50 μM Sephin1.

Cells were washed twice with PBS and fixed with ice-cold 4% PFA for 10 min at RT. Following fixation, cells were washed three times with PBS for 5 min, and then blocked in PBS supplemented with 5% BSA, 1% normal donkey serum (DNS), and 0.1% Triton X-100 for one hour. Primary antibodies were diluted in block solution and incubated at 4^{o}C overnight. The following antibodies were used: Rabbit anti-G3BP1 (Abcam, ab181150, 1:500) and mouse anti-O1 (R&D, MAB1327, 1:500), anti-PDGFR-alpha (BD Biosciences, 558774, 1:100), anti-MBP (Abcam, ab24567, 1:700). Following primary antibody incubation, the cells were washed with PBS and probed with Alexa Fluor-conjugated secondary antibodies (Thermo Fisher Scientific,1:500) for 1hr at RT. Cells were then washed with PBS and mounted using HardSet™ Antifade Mounting Medium with DAPI (VECTASHIELD, H-1500–10). Cells were viewed on a Zeiss LSM 880 confocal microscope.

Op-Puro labeling of cultured cells

OPCs were grown on PDL-coated 4-well glass culture slides in proliferation media overnight. We exposed cells to the differentiation medium supplemented with 200 U/ml IFN-γ, and/or 50 μM Sephin1 for eight hours. 50μm OP-puro (#7391, Tocris) was added to cells for the last one hour. Treatment with 50 μg/mL CHX (#C4859, Sigma) along with OP-puro for one hour was used as a positive control. After incubation, the cells were washed with PBS and then fixed with cold methanol for 2 min at −20°C. After washing with 0.2% Triton X-100 in TBS, 20 mM Alexa568-azide (#1291–1, Click chemical tools) was added to the fixed cells to detect OP-puro incorporated into nascent protein by CuAAC. After staining, cells were then washed with TBST and mounted with HardSet™ Antifade Mounting Medium with DAPI. Nascent protein synthesis was assessed by determination of signal intensity in the red fluorescent channel as determined by a Zeiss LSM 880 confocal microscope. More than 50 cells were quantified per condition.

Histology (immunofluorescent staining and electron microscopy) and imaging

The histology studies were previously described (Chen et al., 2021). In short, cerebellums were harvested first and then the same mice were the perfused with 4% paraformaldehyde (PFA, Electron Microscopy Sciences, Hatfield, PA) in PBS for 15 min. The brains were removed and cut coronally at approximately 1.3 mm before the bregma. The posterior parts of the brains were post-fixed with 4% PFA overnight, embedded in an OCT compound and cryosectioned in a series of 10 μm. The immunostaining protocol is described in Chen et al., 2021. Primary antibodies included the following: anti-MBP (Abcam, ab24567, 1:700), anti-ASPA (Genetex, GTX113389, 1:500), anti-Ki67 (Abcam, AB15580, 1:100),

anti-PDGFR-alpha (BD Biosciences, 558774, 1:100), anti-cc1 (Calbiochem, OP80, 1:200) and anti-p-eIF2α (Abcam, ab32157, 1:500). The fluorescent stained sections were scanned with an Olympus VS-120 slide scanner and quantified by Image J. At least three serial sections of corpus callosum were quantified. The representative fluorescent images were acquired under a Zeiss LSM 880 confocal microscope.

The anterior parts of the brains were immersed in EM buffer for two weeks at 4°C (Chen et al., 2021), then dehydrated in ethanol, cleared in propylene oxide, and embedded in EMBed 812 resin (Electron Microscopy Sciences). Grids were examined on an FEI Tecnai Spirit G2 transmission electron microscope. The total percentage of remyelinated axons, averaged from 10 images (area = 518.3504 μm2) in each mouse, was calculated. G-ratios were calculated as the ratio of the inner diameter to the outer diameter of a myelinated axon; a minimum of 300 fibers per mouse was analyzed.

Quantitative real-time reverse transcription PCR (RT-qPCR)

The RT-qPCR procedure was described previously (Chen et al., 2021). Total RNA was isolated from the cerebellum. RT-qPCR was performed on a CFX96 RT-PCR detection system (Bio-Rad) using SYBR Green technology. Results were analyzed and presented as the fold-induction relative to the internal control primer for the housekeeping gene GAPDH. The primers (5′–3′) for the mouse gene sequences were as follows: Gapdh-f: TGTGTCCGTCGTGGATCTGA, Gapdh-r: TTGCTGTTGAAGTCGCAGGAG; Ifng-f: GATATCTGGAGGAACTGGCAAAA, Ifng-r: CTTCAAAGAGTCTGAGGTAGAAAGAGATAAT.

Super-resolution imaging and processing

Structured illumination microscopy (SIM) images were obtained using a Zeiss Elyra 7 equipped with dual pco.edge 4.2 sCMOS cameras. Collected light split using a Long ass 560 filter and 405, 488, and 561nm laser lines were used for excitation. Images were acquired using Zen Black Software (Zeiss). SIM images were processed using dual iterative reconstruction (SIM2, Zeiss) in Zen Black using Standard Live preset parameters. To analyze the proportion of oligodendrocytes positive for G3BP1 accumulation, images were quantified from widefield images of G3BP1 immunofluorescent staining. Analysis was conducted on images from blinded experimental conditions. Cells positive for G3BP1 accumulation were assessed as those with increased G3BP1 levels in the perinuclear region.

Statistical analysis

All results are expressed as mean±SEM. Statistical significance for these data was determined by t-tests, analysis of variance (ANOVA) followed by Student’s test and the Bonferroni method for multiple group experiments. Significance levels were set at $p < 0.05$.

Supplementary Material

Refer to Web version on PubMed Central for supplementary material.

ACKNOWLEDGEMENTS

We thank Erdong Liu and Nia Stewert from Northwestern University, and Peyton Fay, Kevin Kaschke, and Gwen Schulz from Loyola University for technical assistance, and we thank Dr. Jeff Twiss from the University of South Carolina for advice on detecting RNA stress granules. We thank Inflectis Bioscience for providing Sephin1. This study was supported by NIH/NINDS R01 NS034939 (BP), the Dr. Miriam and Sheldon G. Adelson Medical Research Foundation (JRC and BP), the Rampy MS Research Foundation (JRC and BP), and National Multiple Sclerosis Society Career Transition Fellowship TA-2008-37043 (YC).

DATA AVAILABILITY

The data that support the findings of this study are available from the corresponding author, upon reasonable request.

REFERENCES

Anderson P, and Kedersha N. (2008). Stress granules: the Tao of RNA triage. Trends Biochem. Sci 33, 141–150. [PubMed: 18291657]

Cagnetta R, Wong HH-W, Frese CK, Mallucci GR, Krijgsveld J, and Holt CE (2019). Noncanonical Modulation of the eIF2 Pathway Controls an Increase in Local Translation during Neural Wiring. Mol. Cell 73, 474–489.e5. [PubMed: 30595434]

Carrara M, Sigurdardottir A, and Bertolotti A. (2017). Decoding the selectivity of eIF2α holophosphatases and PPP1R15A inhibitors. Nat. Struct. Mol. Biol 24, 708–716. [PubMed: 28759048]

Chen Y, Podojil JR, Kunjamma RB, Jones J, Weiner M, Lin W, Miller SD, and Popko B. (2019). Sephin1, which prolongs the integrated stress response, is a promising therapeutic for multiple sclerosis. Brain 142, 344–361. [PubMed: 30657878]

Chen Y, Kunjamma RB, Weiner M, Chan JR, and Popko B. (2021). Prolonging the integrated stress response enhances CNS remyelination in an inflammatory environment. Elife 10.

Clayton BLL, and Popko B. (2016). Endoplasmic reticulum stress and the unfolded protein response in disorders of myelinating glia. Brain Res. 1648, 594–602. [PubMed: 27055915]

Compston A, and Coles A. (2002). Multiple sclerosis. Lancet 359, 1221–1231. [PubMed: 11955556]

Costa-Mattioli M, and Walter P. (2020). The integrated stress response: From mechanism to disease. Science 368.

Crespillo-Casado A, Chambers JE, Fischer PM, Marciniak SJ, and Ron D. (2017). PPP1R15A-mediated dephosphorylation of eIF2α is unaffected by Sephin1 or Guanabenz. Elife 6.

Crespillo-Casado A, Claes Z, Choy MS, Peti W, Bollen M, and Ron D. (2018). A Sephin1-insensitive tripartite holophosphatase dephosphorylates translation initiation factor 2α. J. Biol. Chem 293, 7766–7776. [PubMed: 29618508]

Das I, Krzyzosiak A, Schneider K, Wrabetz L, D'Antonio M, Barry N, Sigurdardottir A, and Bertolotti A. (2015). Preventing proteostasis diseases by selective inhibition of a phosphatase regulatory subunit. Science 348, 239–242. [PubMed: 25859045]

Dugas JC, and Emery B. (2013). Purification of oligodendrocyte precursor cells from rat cortices by immunopanning. Cold Spring Harb. Protoc 2013, 745–758. [PubMed: 23906908]

Fancy SPJ, Kotter MR, Harrington EP, Huang JK, Zhao C, Rowitch DH, and Franklin RJM (2010). Overcoming remyelination failure in multiple sclerosis and other myelin disorders. Exp. Neurol 225, 18–23. [PubMed: 20044992]

Franklin RJM, and Ffrench-Constant C. (2008). Remyelination in the CNS: from biology to therapy. Nat. Rev. Neurosci 9, 839–855. [PubMed: 18931697]

Franklin RJM, and Ffrench-Constant C. (2017). Regenerating CNS myelin - from mechanisms to experimental medicines. Nat. Rev. Neurosci 18, 753–769. [PubMed: 29142295]

Franklin RJM, and Goldman SA (2015). Glia Disease and Repair-Remyelination. Cold Spring Harb. Perspect. Biol 7, a020594.

Franklin RJM, and Simons M. (2022). CNS remyelination and inflammation: From basic mechanisms to therapeutic opportunities. Neuron 110, 3549–3565. [PubMed: 36228613]

Franklin RJM, Frisén J, and Lyons DA (2021). Revisiting remyelination: Towards a consensus on the regeneration of CNS myelin. Semin. Cell Dev. Biol 116, 3–9. [PubMed: 33082115]

Frohman EM, Racke MK, and Raine CS (2006). Multiple sclerosis--the plaque and its pathogenesis. N. Engl. J. Med 354, 942–955. [PubMed: 16510748]

Galloway DA, Gowing E, Setayeshgar S, and Kothary R. (2020). Inhibitory milieu at the multiple sclerosis lesion site and the challenges for remyelination. Glia 68, 859–877. [PubMed: 31441132]

Glauninger H, Wong Hickernell CJ, Bard JAM, and Drummond DA (2022). Stressful steps: Progress and challenges in understanding stress-induced mRNA condensation and accumulation in stress granules. Mol. Cell 82, 2544–2556. [PubMed: 35662398]

Goverman J. (2009). Autoimmune T cell responses in the central nervous system. Nat. Rev. Immunol 9, 393–407. [PubMed: 19444307]

Hofmann S, Kedersha N, Anderson P, and Ivanov P. (2021). Molecular mechanisms of stress granule assembly and disassembly. Biochim. Biophys. Acta Mol. Cell Res 1868, 118876. [PubMed: 33007331]

Holcik M, and Sonenberg N. (2005). Translational control in stress and apoptosis. Nat. Rev. Mol. Cell Biol 6, 318–327. [PubMed: 15803138]

Hussien Y, Podojil JR, Robinson AP, Lee AS, Miller SD, and Popko B. (2015). ER Chaperone BiP/GRP78 Is Required for Myelinating Cell Survival and Provides Protection during Experimental Autoimmune Encephalomyelitis. J. Neurosci 35, 15921–15933. [PubMed: 26631473]

Kedersha N, and Anderson P. (2002). Stress granules: sites of mRNA triage that regulate mRNA stability and translatability. Biochem. Soc. Trans 30, 963–969. [PubMed: 12440955]

Kedersha NL, Gupta M, Li W, Miller I, and Anderson P. (1999). RNA-binding proteins TIA-1 and TIAR link the phosphorylation of eIF-2 alpha to the assembly of mammalian stress granules. J. Cell Biol 147, 1431–1442. [PubMed: 10613902]

Khong A, Matheny T, Jain S, Mitchell SF, Wheeler JR, and Parker R. (2017). The Stress Granule Transcriptome Reveals Principles of mRNA Accumulation in Stress Granules. Mol. Cell 68, 808–820.e5. [PubMed: 29129640]

Krishnamoorthy T, Pavitt GD, Zhang F, Dever TE, and Hinnebusch AG (2001). Tight binding of the phosphorylated alpha subunit of initiation factor 2 (eIF2alpha) to the regulatory subunits of guanine nucleotide exchange factor eIF2B is required for inhibition of translation initiation. Mol. Cell. Biol 21, 5018–5030. [PubMed: 11438658]

Lassmann H. (2014). Mechanisms of white matter damage in multiple sclerosis. Glia 62, 1816–1830. [PubMed: 24470325]

Lassmann H. (2018). Pathogenic mechanisms associated with different clinical courses of multiple sclerosis. Front. Immunol 9, 3116. [PubMed: 30687321]

Lees JR, and Cross AH (2007). A little stress is good: IFN-gamma, demyelination, and multiple sclerosis. J. Clin. Invest 117, 297–299. [PubMed: 17273549]

Lin W, and Popko B. (2009). Endoplasmic reticulum stress in disorders of myelinating cells. Nat. Neurosci 12, 379–385. [PubMed: 19287390]

Lin W, Harding HP, Ron D, and Popko B. (2005). Endoplasmic reticulum stress modulates the response of myelinating oligodendrocytes to the immune cytokine interferon-gamma. J. Cell Biol 169, 603–612. [PubMed: 15911877]

Lin W, Kemper A, Dupree JL, Harding HP, Ron D, and Popko B. (2006). Interferon-gamma inhibits central nervous system remyelination through a process modulated by endoplasmic reticulum stress. Brain 129, 1306–1318. [PubMed: 16504972]

Lin W, Bailey SL, Ho H, Harding HP, Ron D, Miller SD, and Popko B. (2007). The integrated stress response prevents demyelination by protecting oligodendrocytes against immune-mediated damage. J. Clin. Invest 117, 448–456. [PubMed: 17273557]

Lin W, Lin Y, Li J, Fenstermaker AG, Way SW, Clayton B, Jamison S, Harding HP, Ron D, and Popko B. (2013). Oligodendrocyte-specific activation of PERK signaling protects mice against experimental autoimmune encephalomyelitis. J. Neurosci 33, 5980–5991. [PubMed: 23554479]

Lin Y, Huang G, Jamison S, Li J, Harding HP, Ron D, and Lin W. (2014). PERK activation preserves the viability and function of remyelinating oligodendrocytes in immune-mediated demyelinating diseases. Am. J. Pathol 184, 507–519. [PubMed: 24269558]

Liu J, Xu Y, Stoleru D, and Salic A. (2012). Imaging protein synthesis in cells and tissues with an alkyne analog of puromycin. Proc. Natl. Acad. Sci. USA 109, 413–418. [PubMed: 22160674]

Lytton J, Westlin M, and Hanley MR (1991). Thapsigargin inhibits the sarcoplasmic or endoplasmic reticulum Ca-ATPase family of calcium pumps. J. Biol. Chem 266, 17067–17071. [PubMed: 1832668]

Mateju D, Eichenberger B, Voigt F, Eglinger J, Roth G, and Chao JA (2020). Single-Molecule Imaging Reveals Translation of mRNAs Localized to Stress Granules. Cell 183, 1801–1812.e13. [PubMed: 33308477]

Mháille AN, McQuaid S, Windebank A, Cunnea P, McMahon J, Samali A, and FitzGerald U. (2008). Increased expression of endoplasmic reticulum stress-related signaling pathway molecules in multiple sclerosis lesions. J. Neuropathol. Exp. Neurol 67, 200–211. [PubMed: 18344911]

Pakos-Zebrucka K, Koryga I, Mnich K, Ljujic M, Samali A, and Gorman AM (2016). The integrated stress response. EMBO Rep. 17, 1374–1395. [PubMed: 27629041]

Patel J, and Balabanov R. (2012). Molecular mechanisms of oligodendrocyte injury in multiple sclerosis and experimental autoimmune encephalomyelitis. Int. J. Mol. Sci 13, 10647–10659. [PubMed: 22949885]

Pavitt GD, and Ron D. (2012). New insights into translational regulation in the endoplasmic reticulum unfolded protein response. Cold Spring Harb. Perspect. Biol 4.

Popko B, Corbin JG, Baerwald KD, Dupree J, and Garcia AM (1997). The effects of interferon-gamma on the central nervous system. Mol. Neurobiol 14, 19–35. [PubMed: 9170099]

Rankin KA, Mei F, Kim K, Shen Y-AA, Mayoral SR, Desponts C, Lorrain DS, Green AJ, Baranzini SE, Chan JR, et al. (2019). Selective estrogen receptor modulators enhance CNS remyelination independent of estrogen receptors. J. Neurosci 39, 2184–2194. [PubMed: 30696729]

Reich DS, Lucchinetti CF, and Calabresi PA (2018). Multiple Sclerosis. N. Engl. J. Med 378, 169–180. [PubMed: 29320652]

Ruffini F, Kennedy TE, and Antel JP (2004). Inflammation and remyelination in the central nervous system: a tale of two systems. Am. J. Pathol 164, 1519–1522. [PubMed: 15111297]

Schmidt EK, Clavarino G, Ceppi M, and Pierre P. (2009). SUnSET, a nonradioactive method to monitor protein synthesis. Nat. Methods 6, 275–277. [PubMed: 19305406]

Schultz V, van der Meer F, Wrzos C, Scheidt U, Bahn E, Stadelmann C, Brück W, and Junker A. (2017). Acutely damaged axons are remyelinated in multiple sclerosis and experimental models of demyelination. Glia 65, 1350–1360. [PubMed: 28560740]

Sehgal P, Szalai P, Olesen C, Praetorius HA, Nissen P, Christensen SB, Engedal N, and Møller JV (2017). Inhibition of the sarco/endoplasmic reticulum (ER) Ca2+-ATPase by thapsigargin analogs induces cell death via ER Ca2+ depletion and the unfolded protein response. J. Biol. Chem 292, 19656–19673. [PubMed: 28972171]

Sidrauski C, Tsai JC, Kampmann M, Hearn BR, Vedantham P, Jaishankar P, Sokabe M, Mendez AS, Newton BW, Tang EL, et al. (2015). Pharmacological dimerization and activation of the exchange factor eIF2B antagonizes the integrated stress response. Elife 4, e07314. [PubMed: 25875391]

Starost L, Lindner M, Herold M, Xu YKT, Drexler HCA, Heβ K, Ehrlich M, Ottoboni L, Ruffini F, Stehling M, et al. (2020). Extrinsic immune cell-derived, but not intrinsic oligodendroglial factors contribute to oligodendroglial differentiation block in multiple sclerosis. Acta Neuropathol. 140, 715–736. [PubMed: 32894330]

Stone S, and Lin W. (2015). The unfolded protein response in multiple sclerosis. Front. Neurosci 9, 264. [PubMed: 26283904]

Stone S, Wu S, Jamison S, Durose W, Pallais JP, and Lin W. (2018). Activating transcription factor 6α deficiency exacerbates oligodendrocyte death and myelin damage in immune-mediated demyelinating diseases. Glia 66, 1331–1345. [PubMed: 29436030]

Titus HE, Chen Y, Podojil JR, Robinson AP, Balabanov R, Popko B, and Miller SD (2020). Pre-clinical and Clinical Implications of “Inside-Out” vs. “Outside-In” Paradigms in Multiple Sclerosis Etiopathogenesis. Front. Cell Neurosci 14, 599717. [PubMed: 33192332]

Tourrière H, Chebli K, Zekri L, Courselaud B, Blanchard JM, Bertrand E, and Tazi J. (2003). The RasGAP-associated endoribonuclease G3BP assembles stress granules. J. Cell Biol 160, 823–831. [PubMed: 12642610]

Volpi VG, Touvier T, and D'Antonio M. (2016). Endoplasmic reticulum protein quality control failure in myelin disorders. Front. Mol. Neurosci 9, 162. [PubMed: 28101003]

Way SW, and Popko B. (2016). Harnessing the integrated stress response for the treatment of multiple sclerosis. Lancet Neurol. 15, 434–443. [PubMed: 26873788]

Way SW, Podojil JR, Clayton BL, Zaremba A, Collins TL, Kunjamma RB, Robinson AP, Brugarolas P, Miller RH, Miller SD, et al. (2015). Pharmaceutical integrated stress response enhancement protects oligodendrocytes and provides a potential multiple sclerosis therapeutic. Nat. Commun 6, 6532. [PubMed: 25766071]

Wong YL, LeBon L, Basso AM, Kohlhaas KL, Nikkel AL, Robb HM, Donnelly-Roberts DL, Prakash J, Swensen AM, Rubinstein ND, et al. (2019). eIF2B activator prevents neurological defects caused by a chronic integrated stress response. Elife 8.

Zhang K, and Kaufman RJ (2008). From endoplasmic-reticulum stress to the inflammatory response. Nature 454, 455–462. [PubMed: 18650916]

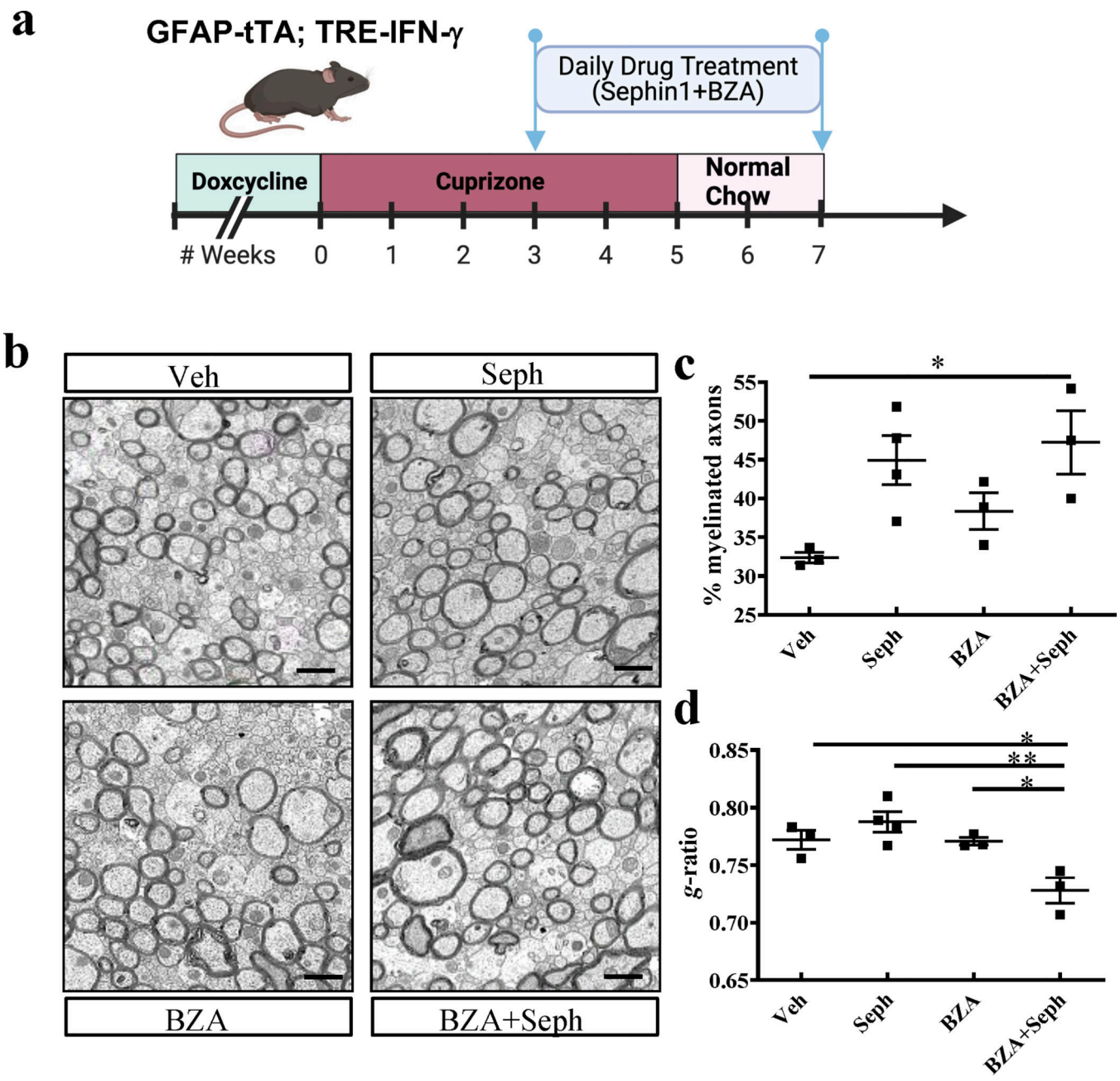

Figure 1. Combined treatment of Sephin1 and BZA promotes early-stage remyelination in the presence of IFN-γ.

(**a**) Cuprizone demyelination/remyelination model of GFAP-tTA;TRE-IFN-γ with designed treatment. Drug treatment was started after three weeks of cuprizone exposure and lasted to the early remyelination stage. (**b**) Corpora callosa of GFAP-tTA;TRE-IFN-γ were taken for EM processing at two weeks after cuprizone withdrawal. Representative EM image of the corpus callosum. Scale bars indicate 1μm. Quantifications of percentage of remyelinated axons (**c**) and g-ratios of axons (**d**) in the corpus callosum areas in the presence of IFN-γ. *p < 0.05, significance based on ANOVA. Data represent an average of 3–4 mice per group (mean ± SEM).

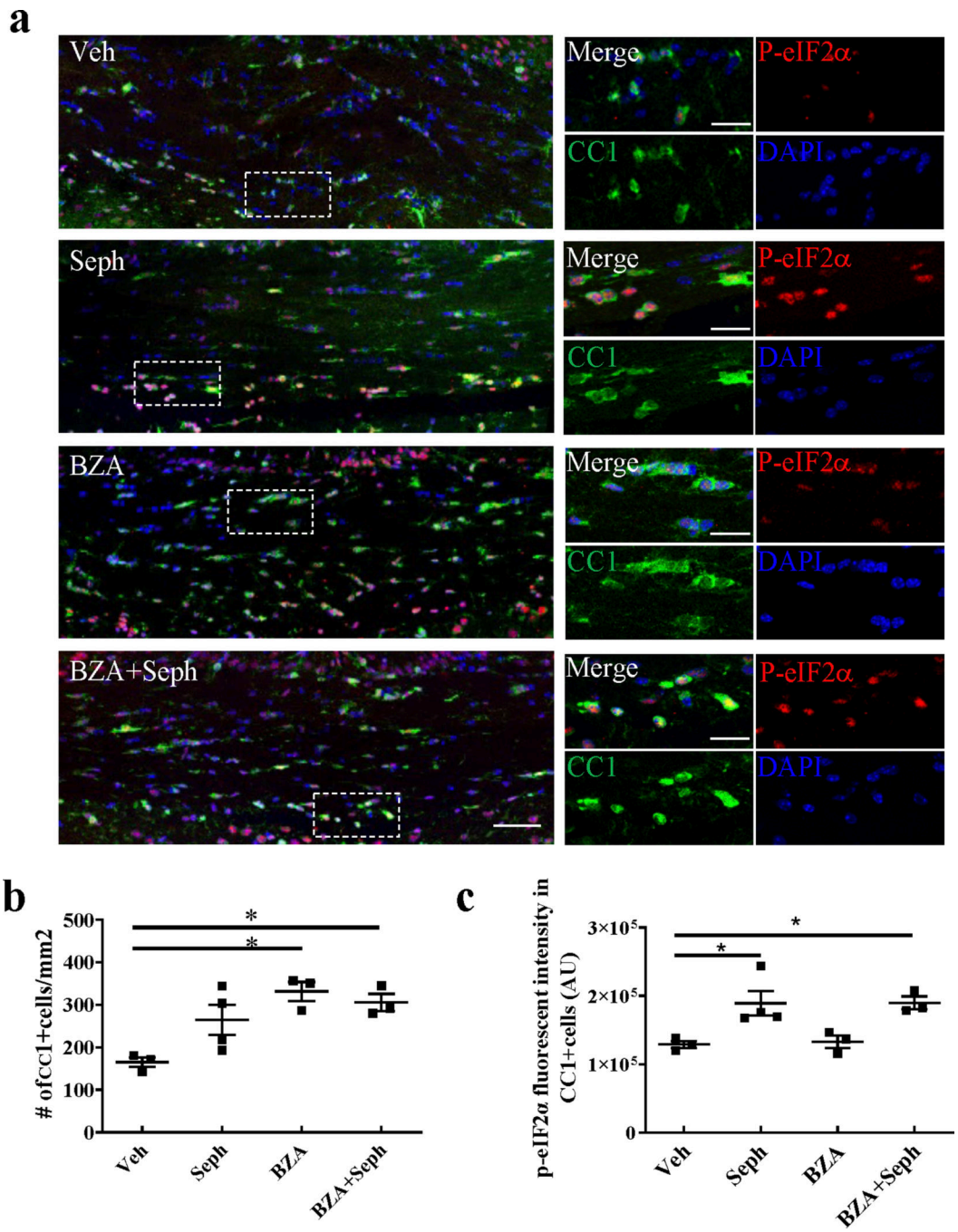

Figure 2. Combined treatment of Sephin1 and BZA increases the number of remyelinating oligodendrocytes in the early-stage remyelination.

(**a**) Immunostaining of the corpus callosum with anti-cc1, anti-p-eIF2α and DAPI. Scale bars indicate 50μm. Higher magnification images are taken from the boxed areas. Scale bars indicate 20 μm. (**b**) Quantification of cells positive for CC1 in the corpus callosum. (**c**) Quantification of the fluorescent intensity of p-eIF2α staining in the CC1+ oligodendrocytes. *$p < 0.05$, significance based on ANOVA. Data represent an average of 3–4 mice per group (mean ± SEM).

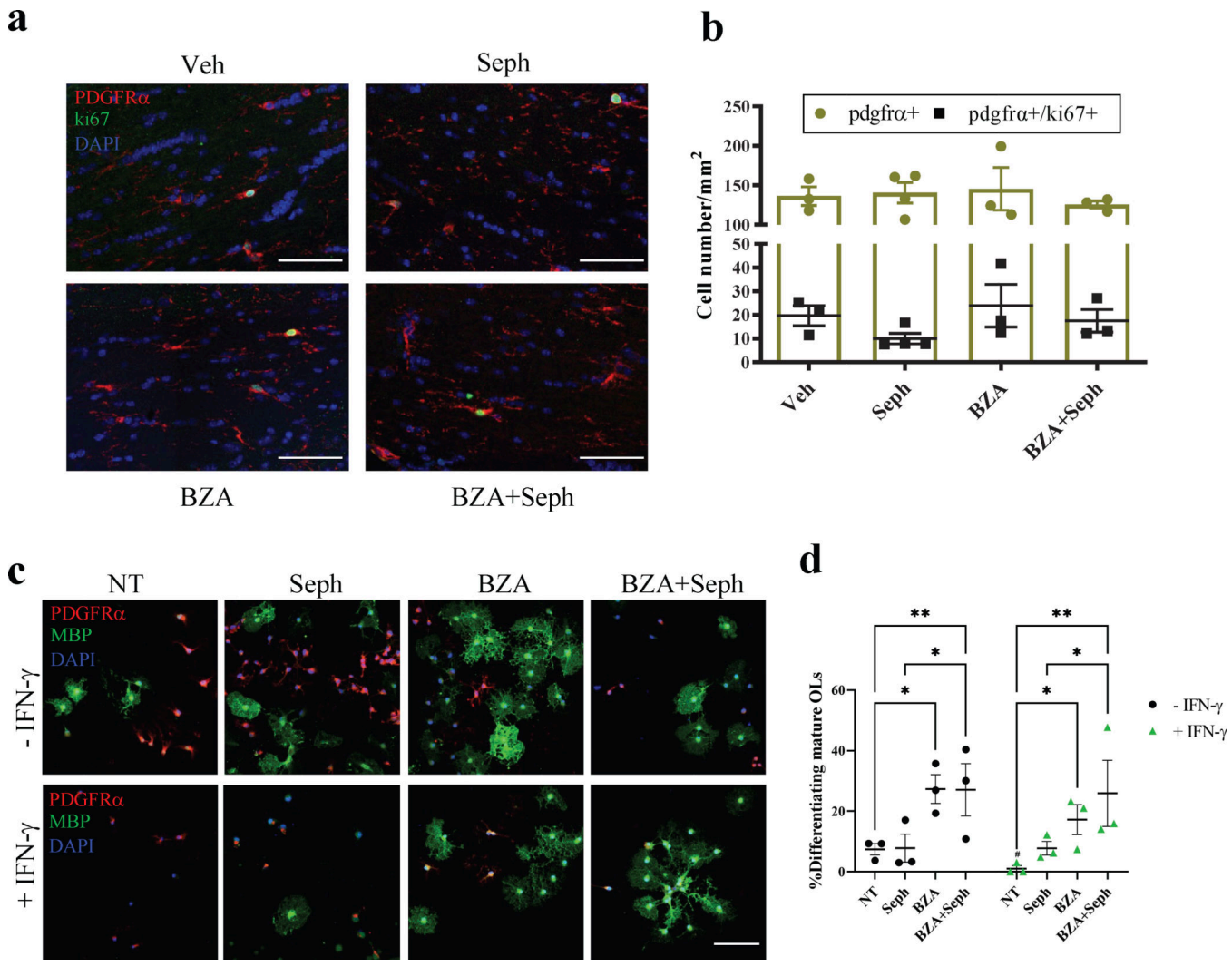

Figure 3. Combined treatment of Sephin1 and BZA does not change OPC proliferation but promotes OPC differentiation.

(**a**) Corpora callosa of GFAP-tTA;TRE-IFN-γ were taken for immunostaining at two weeks after cuprizone withdrawal. Immunostaining of corpus callosum with anti-PDGFR-α, anti-Ki67 and DAPI. Scale bars indicate 50μm. (**b**) Quantification of cells positive for PDGFR-α and cells positive with both PDGFR-α and Ki67 at the corpus callosum. (**c**) PDGFR-α and MBP immunostaining of OPCs in cultures that were seeded for 24 hours. Cells exposed to IFN-γ (+ IFN-γ) were treated with either non-treatment (NT), Sephin1 (Seph), BZA, or BZA plus Sephin1 (BZA+Seph). Cells were not exposed to IFN-γ (-IFN-γ) as controls. Scale bar indicates 100μm. (**d**) Quantification of percentage of cells positive for MBP (differentiating oligodendrocytes) over the total number of oligodendrocyte lineage cells. *p < 0.05, **p < 0.01, significance based on ANOVA.

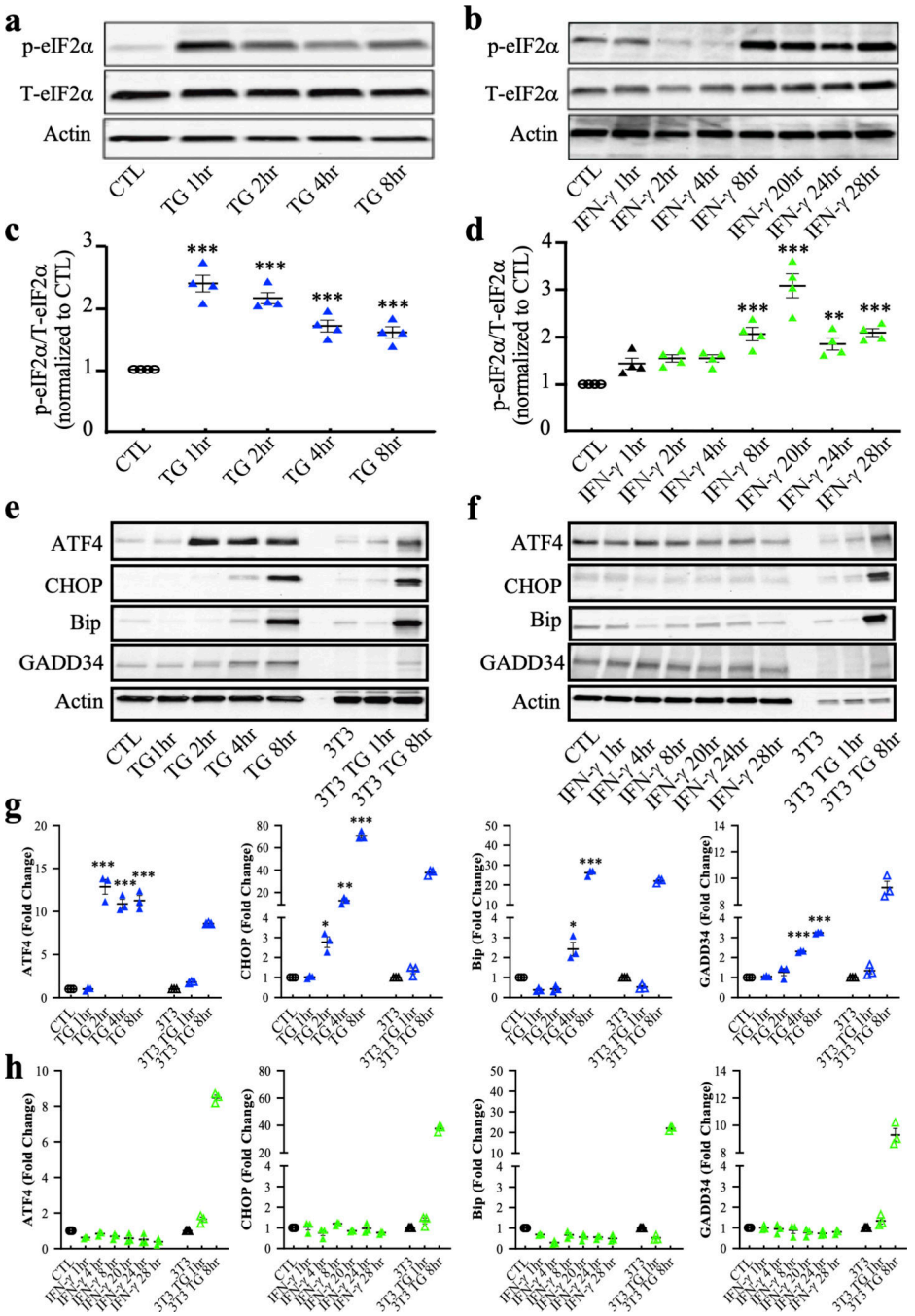

Figure 4. Upregulation of downstream ISR proteins in thapsigargin-treated oligodendrocytes, but not in IFN-γ treated oligodendrocytes.

(a) Immunoblotting analysis of p-eIF2α and total eIF2α in thapsigargin (TG) treated developing oligodendrocytes. **(b)** Immunoblotting analysis of p-eIF2α and total eIF2α in IFN-γ treated developing oligodendrocytes. **(c** and **d)** Quantification of p-eIF2α levels with respect to Western blots **a** and **b**. **(e)** Western blot analysis of the ISR response (ATF4, BIP, GADD34, and CHOP) in TG treated developing oligodendrocytes. **(f)** Western blot analysis of the ISR response in IFN-γ treated developing oligodendrocytes. As a positive

control, NIH 3T3 cells were also incubated with TG for 1 or 8 hrs. (**g** and **h**) Quantification of Western blots **e** and **f**. Data are mean ± SEM. *p < 0.05, **p < 0.01, ***p < 0.001, significance based on ANOVA.

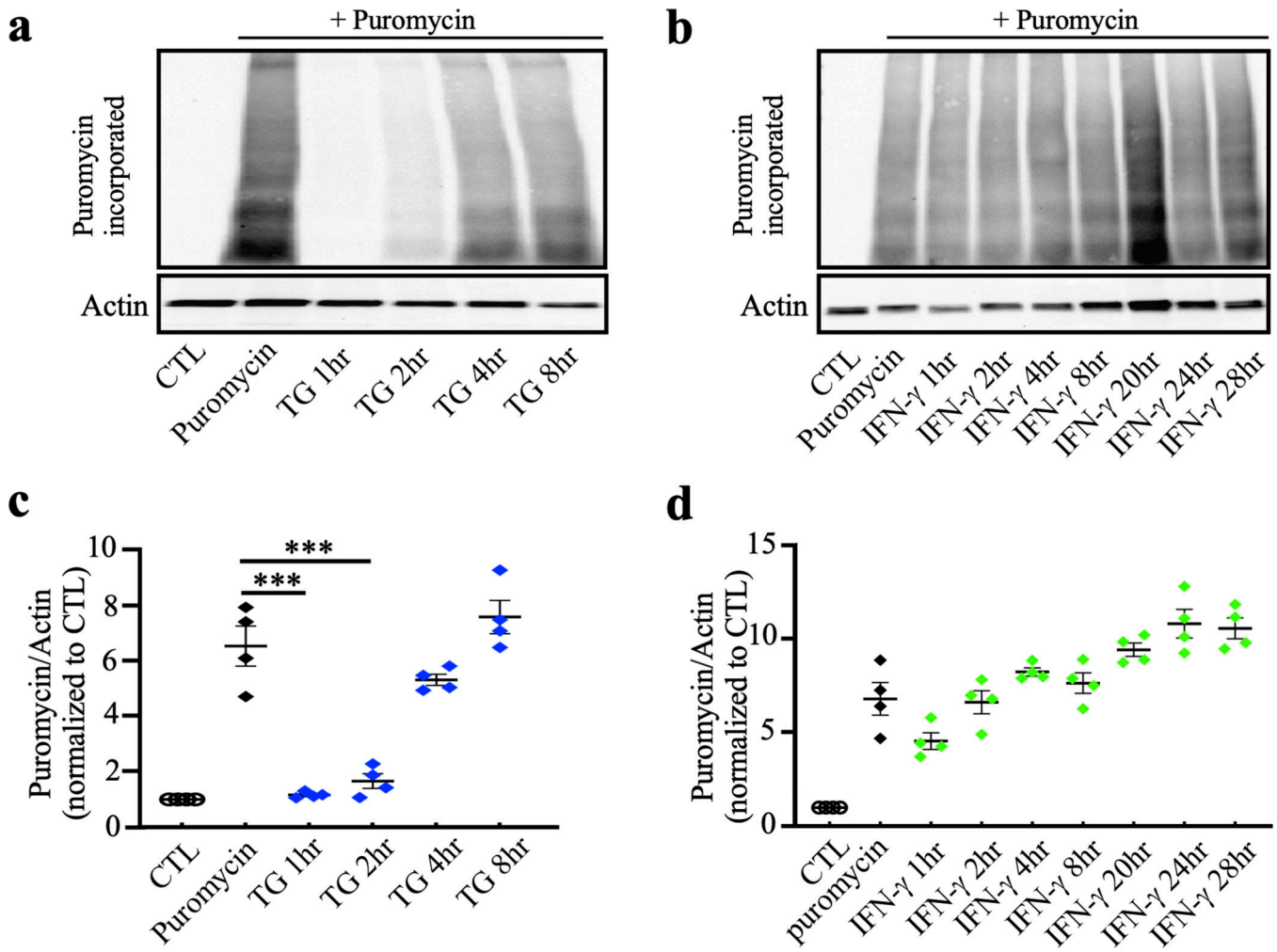

Figure 5. Inhibition of overall cellular protein translation in thapsigargin treated oligodendrocytes, but not in IFN-γ treated oligodendrocytes.

Western blots of puromycin incorporation assay using an anti-puromycin antibody. OPCs were differentiated in differentiation media overnight and then treated with either thapsigargin (TG) **(a)** or IFN-γ **(b)**. Puromycin was added in the last 30 min before harvesting for puromycin labeling. Treatment of puromycin alone served as a positive control. (**c** and **d**) Quantification of Western blots **(a)** and **(b)**. Data are mean ± SEM. ***p < 0.001, significance based on ANOVA.

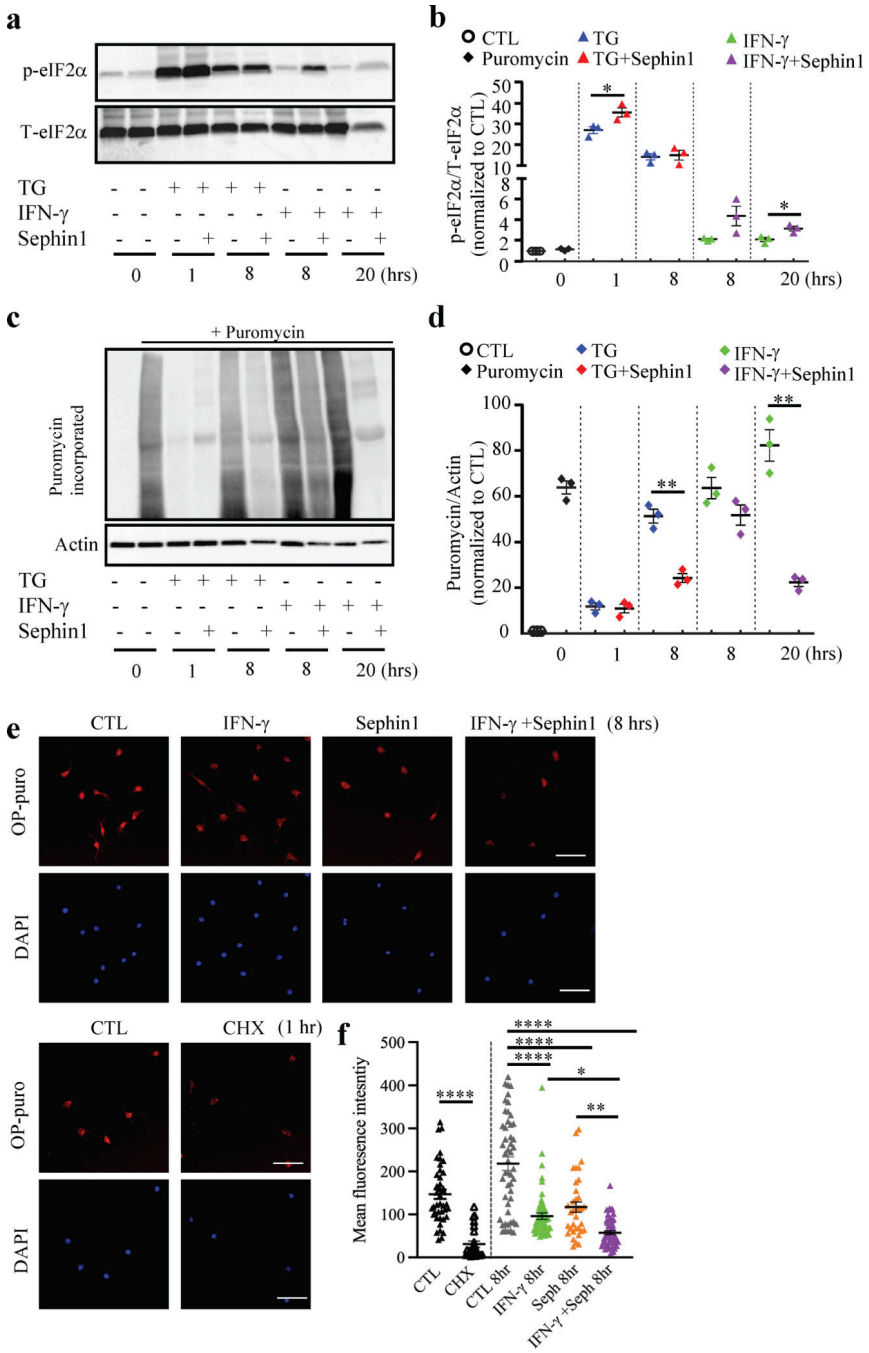

Figure 6. Sephin1 prolongs the ISR response and reduces the overall protein translation in mouse oligodendrocytes.

(a) Western blot of oligodendrocytes treated either by thapsigargin (TG) or IFN-γ with or without Sephin1. **(b)** Quantification of Western blots for p-eIF2α levels. Data are mean ± SEM from three biological isolations and technique replicates. *$p < 0.05$, significance based on unpaired t-test. **(c)** Western blot of puromycin incorporation assay using an anti-puromycin antibody. OPCs were differentiated in differentiation media overnight and then treated with either TG or IFN-γ with or without Sephin1. Puromycin was added in the

last 30 min before harvesting for puromycin labeling. **(d)** Quantification of Western blot in (c). Data are mean ± SEM from three biological isolations and technique replicates. **p < 0.01, significance based on unpaired t-test. **(e)** Imaging nascent proteins in cultured mouse oligodendrocytes. Cultured oligodendrocytes were treated with IFN-γ and/or Sephin1 for 8 hours. Op-puro was added at the last one hour, followed by fixation and staining with Alexa568-azide. Treatment with CHX for 1 hour as a positive control. Scale bars indicate 50 μm. **(f)** Quantification of Alexa568 fluorescence intensity in this experiment. Data are mean ± SEM from more than 50 cells in each condition. *p < 0.05, **p < 0.01, ****p < 0.0001, significance based on ANOVA.

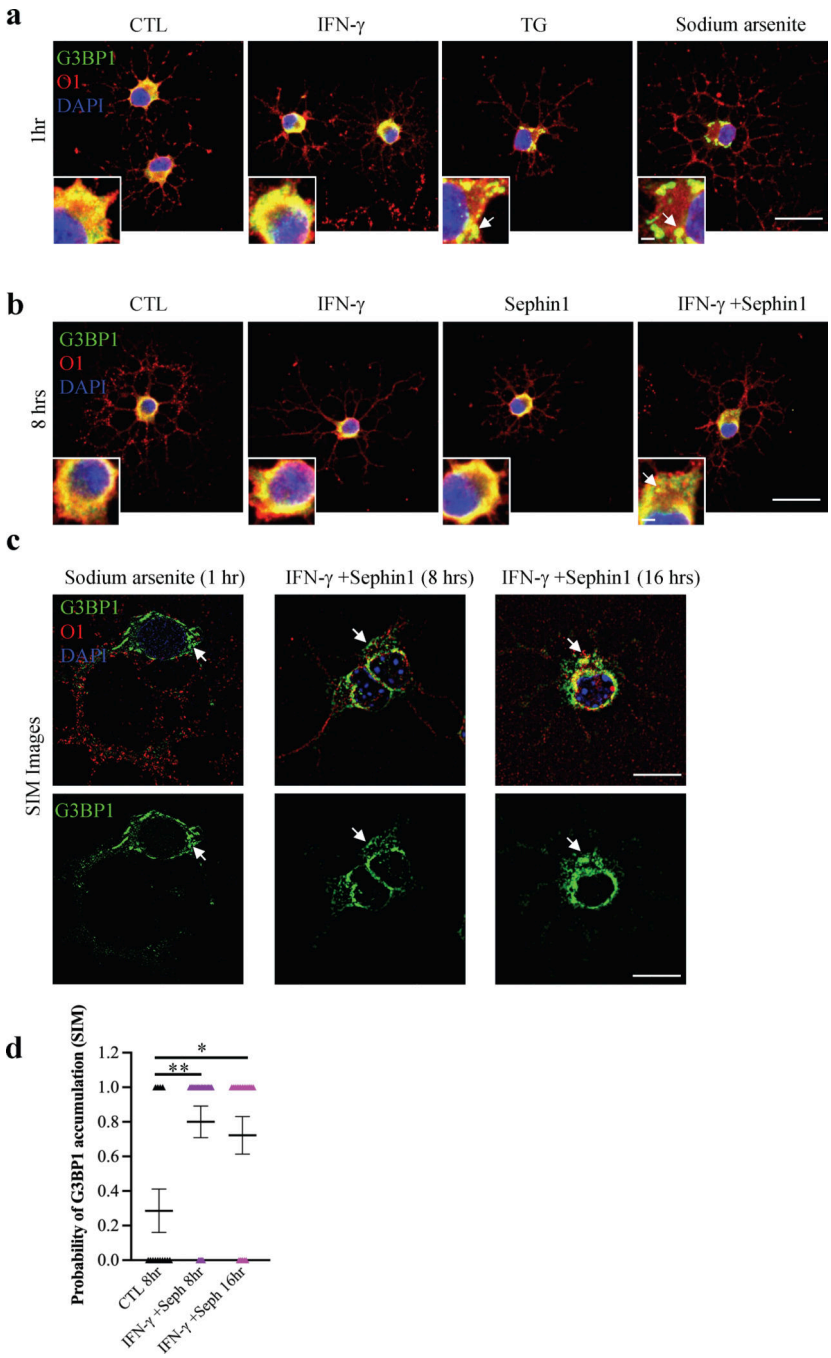

Figure 7. Stress granule formation in IFN-γ stressed oligodendrocytes when treated with Sephin1.

(**a-b**) Representative confocal images of the stress granule marker G3BP1 (green) and oligodendrocyte marker O1 (red) in purified oligodendrocytes. Purified OPCs were incubated in differentiation media overnight and then were either untreated (CTL) or treated with IFN-γ, TG or sodium arsenite for 1 hour (**a**) and 8 hours (**b**). Scale bars indicate 20 μm and 2μm (inserts). White arrows point to G3BP1 puncta. (**c**) Representative SIM images of G3BP1 (green) and O1 (red). Nuclei were stained with DAPI (blue). Scale bars indicate 10

μm. White arrows point to G3BP1 puncta. **(d)** Probability of oligodendrocytes positive for G3BP1 accumulation in different conditions either untreated or treated with 8hr or 16hr dual treatment from SIM images (The presence of G3BP1 accumulation = 1 or the absence=0). N=14 cells (8 hr CTL); N=20 cells (IFN-γ + Seph 8hr); N=18 (IFN-γ + Seph 16hr). Data are mean ± SEM. *p< 0.05; **p<0.01, significance based on ANOVA.

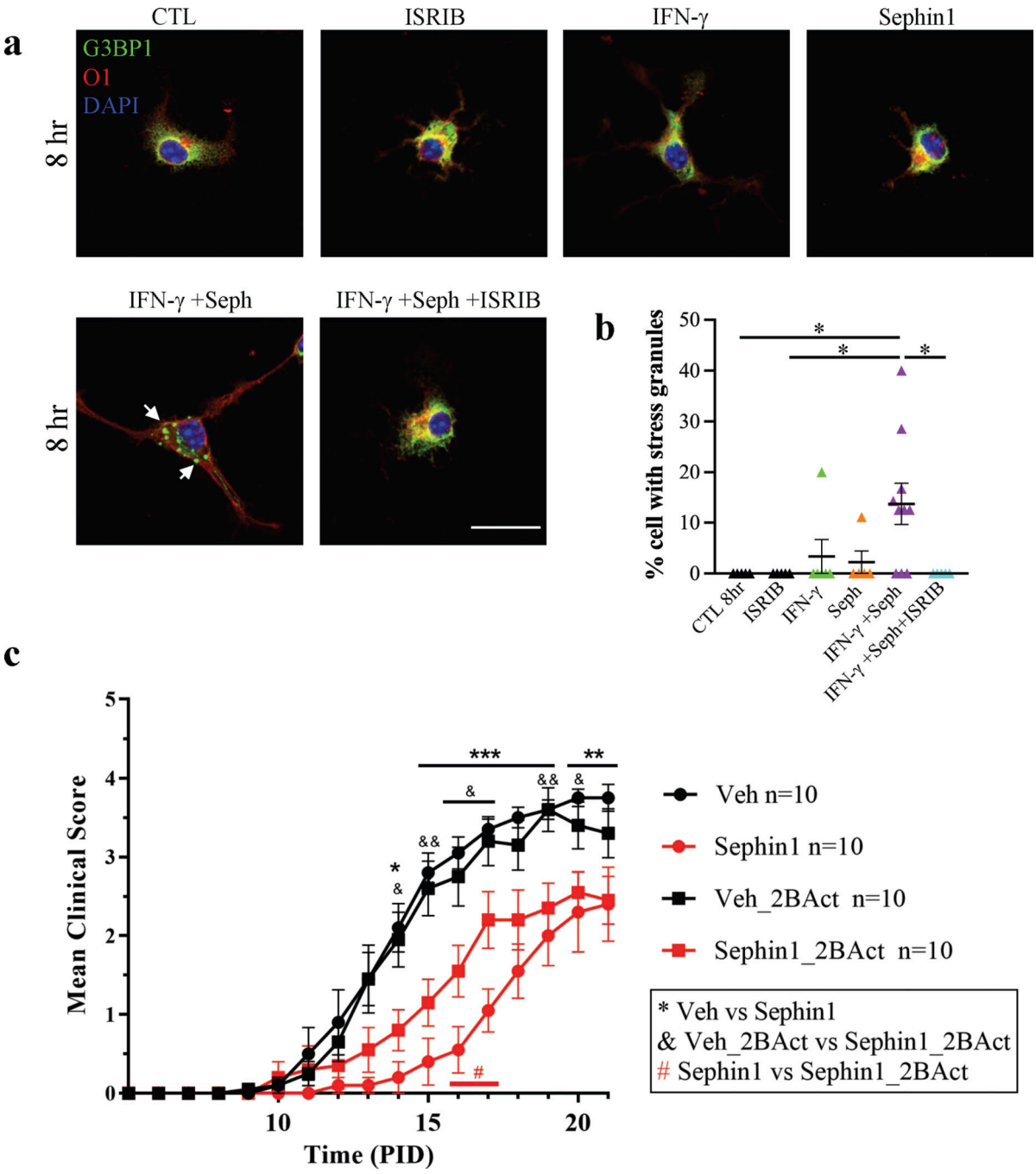

Figure 8. eIF2B activators limit the beneficial effect of Sephin1 on oligodendrocytes.

(a) Representative confocal images of the stress granule marker G3BP1 (green) and oligodendrocyte marker O1 (red) in purified oligodendrocytes. Purified OPCs were incubated in differentiation media overnight and then were either untreated (CTL) or treated with ISRIB, IFN-γ, and/or Sephin1 for 8 hours. White arrows point to G3BP1 puncta. Scale bars indicate 20 μm. **(b)** Quantification of the percentage of cells containing G3BP1 positive stress granules in each condition. Data are mean ± SEM from more than 5 of 20x images in each condition. *p < 0.05, significance based on ANOVA. **(c)** Mean clinical

scores of C57BL/6J female mice immunized with MOG35–55/CFA to induce chronic EAE. Mice were either on normal chow or chow containing 2BAct, treated with vehicle or 8 mg/kg Sephin1. n=10 in each group. *p<0.05, **p<0.01, ***p<0.001; &p<0.05, &&p<0.01. #p<0.05, significance based on ANOVA.